Computers and Geotechnics 69 (2015) 506–513

Contents lists available at ScienceDirect

Computers and Geotechnics

journal homepage: www.elsevier.com/locate/compgeo

Research Paper

Determining an appropriate finite element size for modelling the strength of undrained random soils

J. Huang [a,*], D.V. Griffiths [a,b]

[a] ARC Centre of Excellence for Geotechnical Science and Engineering, The University of Newcastle, NSW, Australia
[b] Colorado School of Mines, Golden, CO, USA

ARTICLE INFO

Article history:
Received 16 January 2015
Received in revised form 19 June 2015
Accepted 23 June 2015

Keywords:
Random field
Discretization error
Finite element method

ABSTRACT

The mechanical properties of soils and rocks can be highly variable, and there has recently been a great deal of interest in modelling this variability using random field theory, in which the material properties vary from point to point. When these point-wise material properties are mapped onto a finite element mesh, discretization errors are inevitable. In this study, the discretization errors are studied and suggestions for element sizes in relation with spatial correlation lengths are given.

1. Introduction

Handling property variability is a research area of great importance and interest in civil, geotechnical and material engineering. At the micro scale, material properties are random due to spatially varied microstructures. Ideally, we would try to directly model this micro scale randomness to predict the overall macro scale performance, but this is obviously too computationally demanding to be practical. A compromise is to use a meso scale, i.e., the size of an element in a finite element method (FEM) simulation by homogenizing the micro scale randomness in each element to predict macro scale performance. When the meso scale is large enough to include all of the micro randomness, the overall material properties at the meso scale are spatially constant. For example, steel usually exhibits randomness on the micrometer scale, but typical finite elements with a size on the order of a centimeter are large enough to have constant properties. In geotechnical engineering, however, the material properties on the meso scale can show significant spatial variability. Random field theory is often used to model spatial variability. The starting point for a discussion of random field modelling is the "point" statistics that are assumed for the model. These are the hypothetical statistical properties of the soil or rock that would be measured if many tests could be performed on infinitesimal samples at a site or laboratory. A convenient measure of the spatial variability of a random field is the correlation length θ. Loosely speaking, θ is the distance within which points are significantly correlated (i.e., by more than approximately 10%). Conversely, two points separated by a distance greater than θ are largely uncorrelated. Many studies have been undertaken in recent years to develop probabilistic methods that address spatial variability in a systematic way (e.g., [9,19,11,13,14,16,1,21,18,17,20]). Of particular importance has been the development of the random finite element method (RFEM) for modelling the spatial variability of geomaterials (e.g., [7]). While mesh effects have been investigated for highly variable materials by some investigators (e.g., [8,5,6,13,14,2,4,15]), the discretization error due to the element size has received little formal attention; the work of with Ching and Phoon [3] is an exception. A small correlation length means that the properties of a soil change rapidly from place to place; therefore, the element size should be small enough to capture the spatial randomness of the material properties. The major aim of the present work, therefore, is to establish a more formal link between the maximum element size and the spatial correlation length. The paper begins with a review of the local averaging method based on the geometric mean. The local averaging method can provide an analytical estimate of the effective overall property by taking the spatial correlation structure into account. Although the geometric mean is dominated by low values, it ignores the "seeking out" effect of a failure mechanism. This effect will be examined using direct Monte Carlo simulations. From the direct simulations, the discretization errors are studied and suggestions for appropriate element sizes in relation with spatial correlation lengths are given.

* Corresponding author.

http://dx.doi.org/10.1016/j.compgeo.2015.06.020
0266-352X/

2. Modelling the strength of materials using local averaging

For the purpose of demonstration, this study will focus on the strengths of engineering materials. It is assumed that the strengths of materials are modelled by point-wise random fields. The question is how small the element size should be for a given spatial correlation length. We restrict ourselves to isotropic Gaussian random fields or random fields that can easily be transformed into Gaussian random fields. We want to investigate the strength in a certain domain (i.e., the macroscale strength) in which the strength at any micro-scale point within the domain is modelled by a random field. In this section, the overall strength of a certain domain is estimated analytically using local averaging. The results will be compared to those of RFEM simulations.

The overall strength of a material in a certain domain is usually dominated by its low-strength regions. Because it is dominated by low values, the geometric mean is recommended by Fenton and Griffiths [7] for estimating the overall strength. The geometric mean is defined as the nth root of the product of n (nonnegative) random variables. Using this definition, the discrete set of random variables $X_1, X_2, \ldots, X_n$ has the geometric mean

$$X_G = (X_1, X_2, \ldots, X_n)^{1/n}. \tag{1}$$

X_G weights low values more heavily than high values (low values dominate). This can be seen by considering what happens to the geometric mean (see Eq. (1)) if even a single X_i is zero: X_G becomes zero.

By expressing Eq. (1) as a power of e, we obtain an alternative way of computing the geometric mean,

$$X_G = \exp\left(\frac{1}{n}\sum_{i=1}^{n} \ln X_i\right). \tag{2}$$

If X is a 1D continuously varying spatial random field, the geometric mean of X over a given domain becomes

$$X_G = \exp\left(\frac{1}{R}\int_0^R \ln X(\xi)d\xi\right), \tag{3}$$

where R is the length over which X is averaged and ξ is a spatial coordinate.

If X is log-normally distributed, X_G tends to be log-normally distributed, according to the central limit theorem. The mean and variance of X_G are found by first finding the mean and variance of $\ln X_G$. The mean of $\ln X_G$ is

$$\begin{aligned} E[\ln X_G] &= E[\tfrac{1}{R}\textstyle\int_0^R \ln X(\xi)d\xi] \\ &= \tfrac{1}{R}\textstyle\int_0^R E[\ln X(\xi)]d\xi \\ &= E[\ln X] \\ &= \mu_{\ln X} \end{aligned} \tag{4}$$

where $\mu_{\ln X}$ is the mean of $\ln X$,

$$\mu_{\ln X} = \ln \mu_X - \frac{1}{2}\sigma^2_{\ln X} \tag{5}$$

and

$$\sigma_{\ln X} = \sqrt{\ln\left(1 + \left(\frac{\sigma_X}{\mu_X}\right)^2\right)}, \tag{6}$$

where μ_X and σ_X are the mean and standard deviation of a log-normally distributed random field X.

We note that because the median of a log-normally distributed random field X is $\exp(\mu_{\ln X})$, the median of X_G is equal to the median of X. In other words, taking the geometric average of a log-normally distributed random field X preserves both the type of distribution and its median.

The variance of $\ln X_G$ is

$$\begin{aligned} \mathrm{Var}\,[\ln X_G] &= E\left[\tfrac{1}{R}\textstyle\int_0^R [\ln X(\xi) - \mu_{\ln X}]d\xi \tfrac{1}{R}\int_0^R [\ln X(\eta) - \mu_{\ln X}]d\eta\right] \\ &= \tfrac{1}{R^2}\textstyle\int_0^R\int_0^R E[(\ln X(\xi) - \mu_{\ln X})(\ln X(\eta) - \mu_{\ln X})]d\xi d\eta \\ &= \tfrac{1}{R^2}\textstyle\int_0^R\int_0^R C_{\ln X}(\tau)(\xi - \eta)d\xi d\eta \\ &= \tfrac{\sigma^2_{\ln X}}{R^2}\textstyle\int_0^R\int_0^R \rho_{\ln X}(\tau)(\xi - \eta)d\xi d\eta \\ &= \sigma^2_{\ln X}\gamma_{\ln X}(R) \end{aligned} \tag{7}$$

where ζ and η are spatial coordinates, τ is the distance between two points, $C_{\ln X}(\tau)$ is the covariance function of $\ln X$, $\rho_{\ln X}(\tau)$ is the correlation function of $\ln X$ such that $C_{\ln X}(\tau) = \sigma^2_{\ln X}\rho_{\ln X}(\tau)$, $\sigma_{\ln X}$ is the mean and standard deviation of $\ln X$, and $\gamma_{\ln X}(R)$ is the variance function that determines how much the variance is reduced when X is averaged over a length R using Eq. (1),

$$\gamma_{\ln X}(R) = \frac{1}{R^2}\int_0^R\int_0^R \rho_{\ln X}(\tau)(\xi - \eta)d\xi d\eta \tag{8}$$

There are a few commonly used correlation functions (see, e.g., [7]). The Markov correlation function used in this study is

$$\rho_{\ln X}(\tau) = \exp\left(-\frac{|\tau|}{\theta_{\ln X}}\right), \tag{9}$$

where $\theta_{\ln X}$ is the spatial correlation length of $\ln X$.

The correlation function in logarithmic space can be converted to the following correlation function in real space (e.g., [25]):

$$\rho_X(\tau) = \frac{\exp(\sigma^2_{\ln X}\rho_{\ln X}(\tau)) - 1}{\exp(\sigma^2_{\ln X}) - 1} \tag{10}$$

For most random fields, the two correlation functions are quite similar and

$$\theta_{\ln X} = \theta_X \tag{11}$$

Because of Eq. (11), from now on, the spatial correlation lengths in the logarithmic and real spaces are both denoted by θ.

In 2D, for a rectangular domain with side lengths R_x and R_y, the variance function is defined by

$$\gamma_{\ln X}(R_x, R_y) = \frac{4}{R_x^2 R_y^2}\int_0^{R_y}\int_0^{R_x} (R_x - x)(R_y - y)\rho_{\ln X}(\tau)\,dx\,dy. \tag{12}$$

Using the correlation function given in Eq. (9), the variance function can be obtained analytically as follows:

$$\gamma_{\ln X}(R_x, R_y) = \frac{4\theta^4}{R_x^2 R_y^2}\left[\frac{R_x}{\theta} + \exp\left(-\frac{R_x}{\theta}\right) - 1\right]\left[\frac{R_y}{\theta} + \exp\left(-\frac{R_y}{\theta}\right) - 1\right], \tag{13}$$

where R_x and R_y are the lengths of the sides of a rectangular domain.

Once the mean and variance of $\ln X_G$ have been computed, the mean and variance of X_G can be computed using

$$\begin{aligned} \mu_{X_G} &= \exp\left(\mu_{\ln X} + \tfrac{1}{2}\sigma^2_{\ln X}\gamma_{\ln X}\right) \\ &= \frac{\mu_X}{\sqrt{\left(1 + \left(\frac{\sigma_X}{\mu_X}\right)^2\right)^{1-\gamma_{\ln X}}}} \end{aligned} \tag{14}$$

and

$$\begin{aligned} \sigma_{X_G} &= \mu_{X_G}\sqrt{\exp(\sigma^2_{\ln X}\gamma_{\ln X} - 1)} \\ &= \mu_{X_G}\sqrt{\exp\left(\ln\left(1 + \left(\frac{\sigma_X}{\mu_X}\right)^2\right)\gamma_{\ln X} - 1\right)} \end{aligned} \tag{15}$$

Eqs. (14) and (15) provide the mean and standard deviation of the locally averaged strength using the geometric mean. It is clear from Eq. (14) that the mean of the locally averaged strength is reduced. It is less obvious from Eq. (15) whether the variance of the locally averaged strength is reduced or not but because the variance of $\ln X_G$ is reduced by local averaging (e.g., Eq. (8)), the variance of the locally averaged strength X_G is also reduced. This can be seen by comparing Eq. (15) and Eq. (16)

$$\sigma_X = \mu_{\ln X}\sqrt{\exp(\sigma^2_{\ln X} - 1)}, \tag{16}$$

where because $\mu_{X_G} < \mu_X$ and $\gamma_{\ln X} < 1$, it follows that $\sigma_{X_G} < \sigma_X$.

For a rectangular domain with side lengths $R_x = L$ and $R_y = 2L$, the mean and standard deviation of the locally averaged strength are shown in Table 1. For comparison, the results for a smaller domain with side lengths $R_x = L$ and $R_y = L$ are also shown in Table 1. It can be seen from Table 1 that a larger domain results in higher reductions in the mean and standard deviation of the locally averaged strength.

3. Modelling the strength of materials using simulations

In an RFEM strength analysis, the failure mechanism occurs naturally as it "seeks out" the weakest path through the soil [9]. The overall strength of a certain domain may be different from the locally averaged values. In this study, biaxial compression tests are performed on a rectangular domain to investigate the macro scale strength for different mesh densities and spatial correlation lengths. The overall strength of the domain is computed using the elastic-plastic finite element method. To reach this goal, an appropriate random field generation technique must be adopted. There are several random field generation techniques available (see e.g., [7]). The Karhunen–Loève (K–L) expansion method (e.g., [23,26]) was chosen for this study because it does not require spatial discretization at the random field generation stage. In the K–L expansion method, the background random fields are generated first; then, values at particular locations can be calculated according to their coordinates. This allows us to compare meshes and study discretization errors. The K–L expansion method represents a random field as an infinite linear combination of the eigenfunctions of the covariance function. Because the series must be truncated to a finite number of terms, a significant concern is that the simulated variance will be reduced. To control this reduction, the eigenvalues are sorted in descending order and the number of terms is determined when the eigenvalues have decayed sufficiently (e.g., [16]).

The domain is axially loaded until it fails under undrained conditions. The undrained shear strength within an element is assumed to be log-normally distributed (*i.e.* $\ln c_u$ is normally distributed) and modelled as a random field. The mean and standard deviation of the undrained shear strength (c_u) are $\mu_{c_u} = 40.0$ kPa and $\sigma_{c_u} = 20.0$ kPa, respectively. The Young's modulus and Poisson's ratio are set to 10^5 kPa and 0.4, respectively. As shown in Fig. 1, the domain has a width of $L = 1.0$ m and a height of $2L$ and is confined isotropically to 10 kPa prior to axial loading, which is applied by incrementing the vertical displacement of the top nodes by 10^{-7} m. The horizontal displacement of the top nodes is not restricted; therefore, the model is of a smooth, rigid loading platen. The mesh consists of eight-node plane strain elements with reduced integration. The return mapping algorithm described by Huang and Griffiths [12] was used. The axial stress at failure, determined based on the mean strength and the Tresca failure criterion, is 90.0 kPa.

To determine how the failure patterns change with the mesh density, typical results for different spatial correlation lengths ($\theta = \{L/8, L/4. L/2. L, 2L\}$) were analyzed. Square elements were used with side length l chosen from $\{L, L/2, L/4, L/8, L/16, L/32, L/64, L/128\}$ m. A random field representing the undrained shear strength was generated at each Gauss point (4 per element) based on its coordinates, as shown in Figs. 2–6. Because the results of direct simulations will be compared to the analytical estimates of the local averages, no local averaging was considered in the direct simulations. Each square represents the zone of influence of one Gauss point (not an element). It may be noted from Figs. 2–6 that the random fields generated using the K–L expansion have a striped pattern, especially when the spatial correlation length is large. This is because the exponential covariance function was decomposed into the product of two 1D eigenfunctions. Figs. 2–6 also show typical failure patterns for different mesh densities and spatial correlation lengths. The densest mesh ($l = L/128$) presumably comes the closest to showing a realistic failure pattern. It is interesting to note that using the coarsest mesh ($l = L/8$) results in a failure pattern that is reasonably consistent with that resulting from using the densest mesh; this holds for all of the spatial correlation lengths considered. It should be mentioned that this observation is based on a single simulation. The failure pattern may change from simulation to simulation. Figs. 7 and 8 show the load–displacement relationship for $\theta = L/4$ (Fig. 3) and $\theta = 2L$ (Fig. 6) for a typical simulation. There are two potential sources of discretization error. One is the discretization of the finite

Table 1
The mean and standard deviation of the locally averaged strength.

θ/L	$R_x = L, R_y = 2L$			$R_x = L, R_y = L$		
	$\gamma_{\ln X}(R_x, R_y)$	μ_{X_G}/μ_X	σ_{X_G}/σ_X	$\gamma_{\ln X}(R_x, R_y)$	μ_{X_G}/μ_X	σ_{X_G}/σ_X
0.125	0.0256	0.8970	0.1359	0.0479	0.8992	0.1863
0.25	0.0825	0.9027	0.2461	0.1423	0.9087	0.3265
0.5	0.2142	0.9161	0.4054	0.3222	0.9272	0.5063
1.0	0.4177	0.9371	0.5858	0.5413	0.9501	0.6809
2.0	0.6270	0.9592	0.7435	0.7263	0.9699	0.8137
4.0	0.7855	0.9763	0.8547	0.8494	0.9833	0.8984
8.0	0.8844	0.9872	0.9222	0.9208	0.9912	0.9468
16.0	0.9399	0.9933	0.9597	0.9594	0.9955	0.9728
32.0	0.9694	0.9966	0.9795	0.9794	0.9977	0.9862
64.0	0.9845	0.9983	0.9896	0.9897	0.9988	0.9931
128.0	0.9922	0.9991	0.9948	0.9948	0.9994	0.9965
256.0	0.9961	0.9996	0.9974	0.9974	0.9997	0.9983

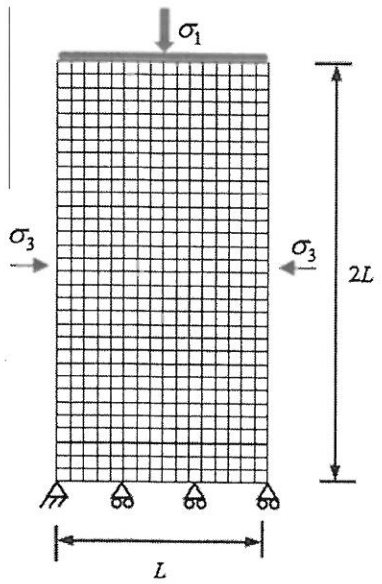

Fig. 1. A biaxial test with smooth, rigid end platens.

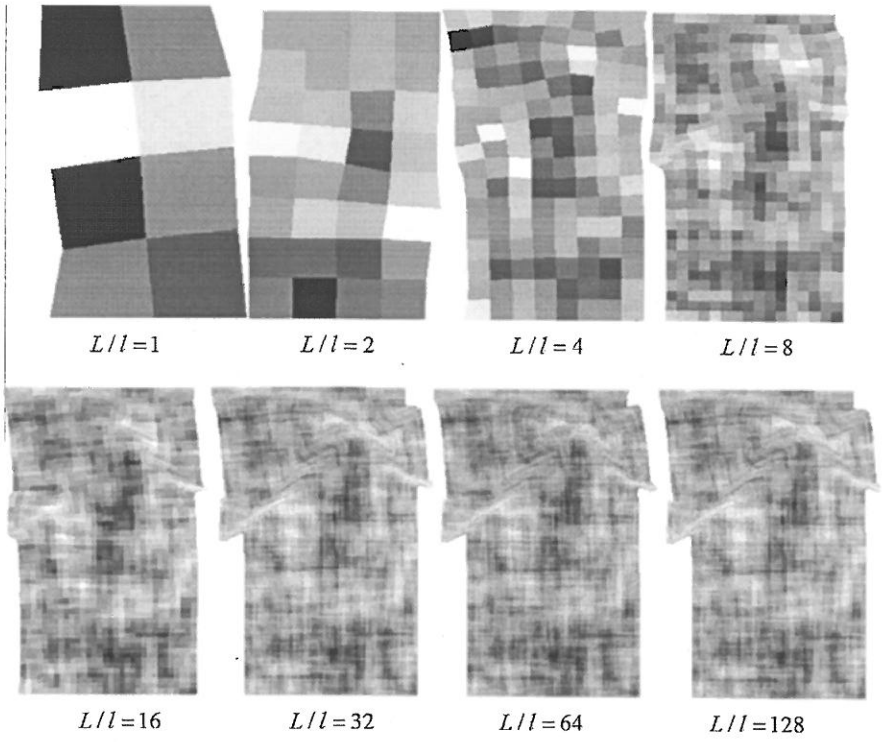

Fig. 2. The deformation at failure ($\theta = L/8$).

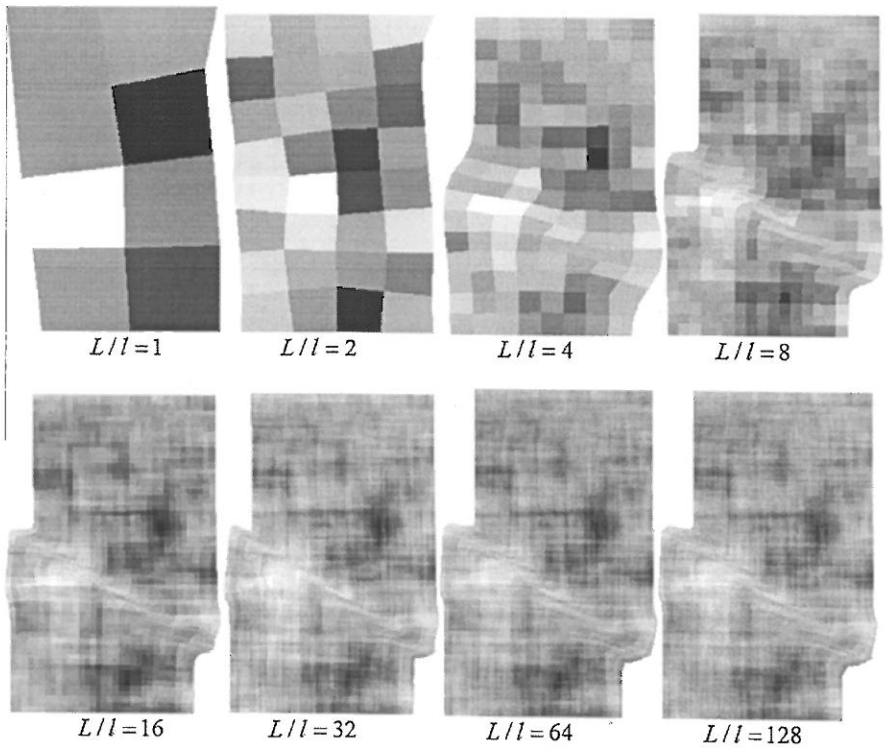

Fig. 3. The deformation at failure ($\theta = L/4$).

element mesh and the other is the discretization of the random field (e.g., [24]). Because the FEM mesh and the random field are often discretized in the same way, these two sources of discretization error are not distinguished in this study. A more comprehensive study should adapt the mesh according to both the random field and the failure mechanism. This is currently being undertaken by the authors and their colleagues using adaptive finite element limit analysis (e.g., [22]).

In Figs. 7 and 8, the loads were back-calculated from the vertical normal stresses in the top row of Gauss points. The failure loads are

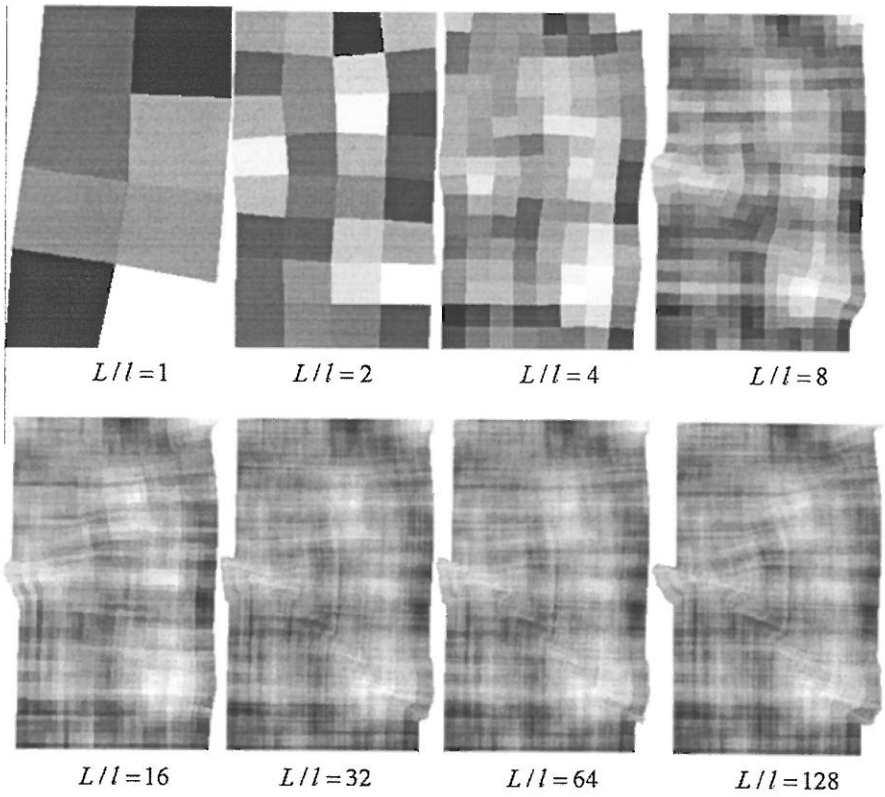

Fig. 4. The deformation at failure ($\theta = L/2$).

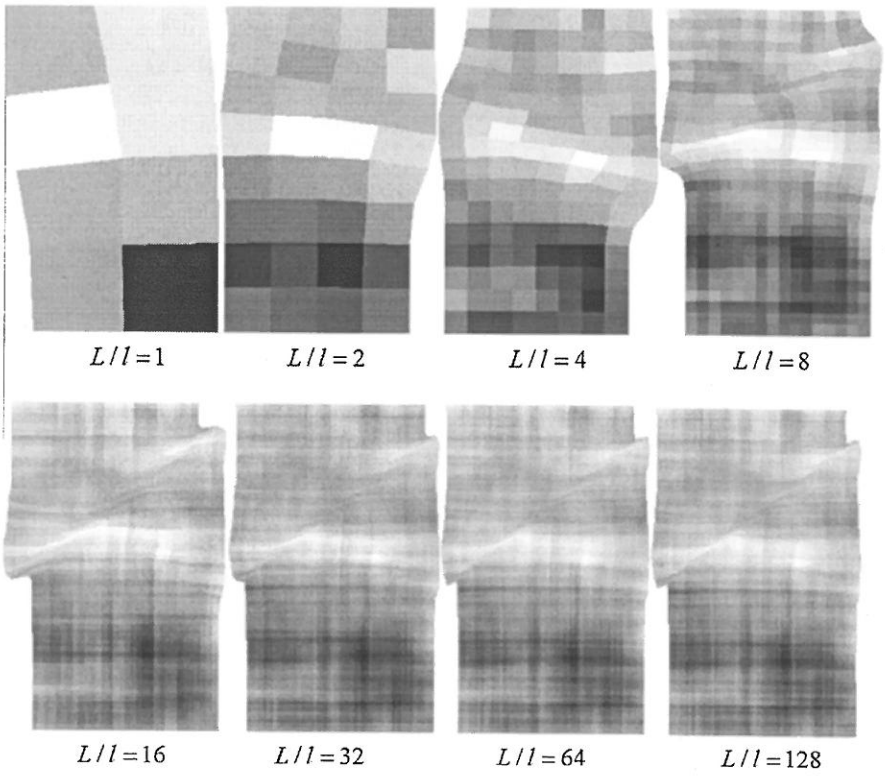

Fig. 5. The deformation at failure ($\theta = L$).

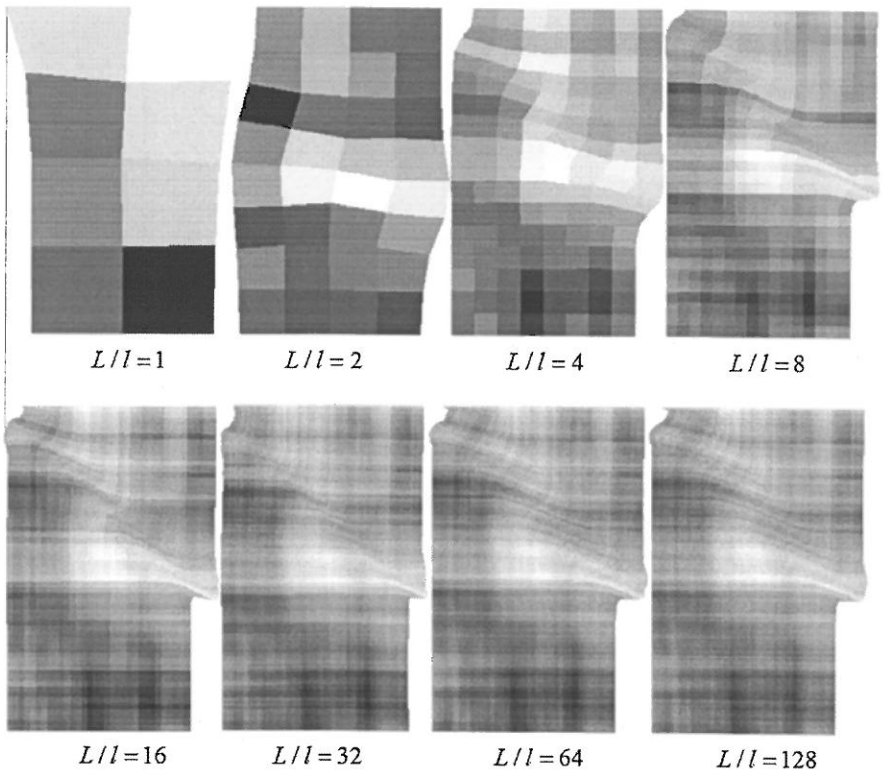

Fig. 6. The deformation at failure ($\theta = 2L$).

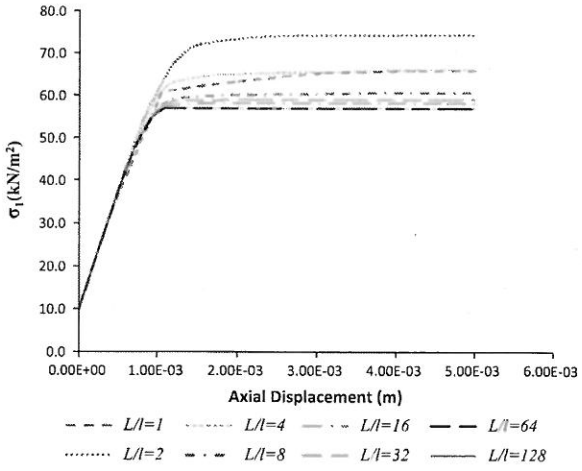

Fig. 7. Axial stress versus axial displacement (corresponding to Fig. 3, $\theta = L/4$).

all less than 90.0 kPa, which is expected because weak elements normally dominate the solution and allow the mechanism to "seek out" a path through the soil.

Fig. 9 shows how the failure load changes with the element size. To achieve a constant failure load, unlike a failure pattern, the element size should be less than $L/32$, but the elements could be larger for higher spatial correlation lengths.

Further investigations into the overall strength were performed using Monte Carlo simulations. For each combination of mesh density and spatial correlation length, two thousand simulations were performed. In each simulation, the overall undrained shear strength was calculated using

$$c_u = \frac{1}{2}(\sigma_{1f} - 10), \tag{17}$$

where σ_{1f} is the failure load. For the example presented, the units of σ_{1f} and c_u are kPa.

The mean and standard deviation of the overall undrained shear strength in two thousand simulations are shown in Figs. 10 and 11. In Figs. 10 and 11, the mean and standard deviation of computed overall shear strength have been normalized by the input mean and the standard deviation of the undrained shear strength, respectively. Fig. 10 shows that the computed mean overall strength is always less than the input mean undrained shear strength, except for very large spatial correlation lengths $\theta > 128L$.

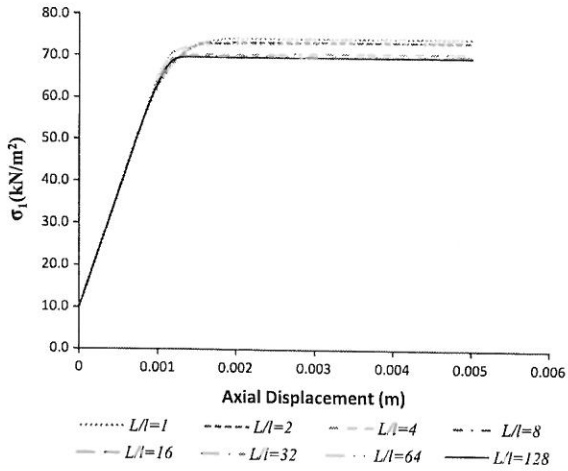

Fig. 8. Axial stress versus axial displacement (corresponding to Fig. 6, $\theta = 2L$).

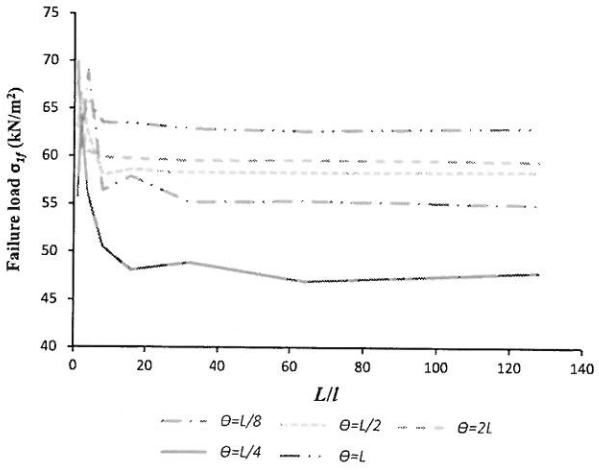

Fig. 9. Failure load versus element size for single simulations (corresponding to Figs. 2–6).

When $\theta > 2L$, the overall mean strength can be estimated well using a coarse mesh with $l = L$. For large spatial correlation lengths $\theta > 2L$, the element size makes virtually no difference. For small spatial correlation lengths $\theta \leq 2L$, the maximum element size that can be used to estimate the mean overall strength reasonably is $l = L/16$. For the smallest spatial correlation length considered, $\theta = L/8$, the maximum element size should, therefore, be less than half of the spatial correlation length. It is also interesting to note that, in this study, the mean overall undrained shear strength is minimized at $\theta = L$. This is often the case in failure studies: the most critical spatial correlation length is often equal to the typical dimension of the studied system (see, e.g., [10]). This means that the element size could be cautiously increased to $\theta = L$ to reduce the computational cost and ensure a conservative result. The standard deviation of the overall strength is shown in Fig. 11.

For the problem considered in this study, which assumes $R_x = L$ and $R_y = 2L$, the mean and standard deviation of the locally averaged strength calculated using Eqs. (14) and (15) are compared to the simulated values given in Fig. 11. Fig. 11 shows that the mean simulated overall strength is always less than the analytically estimated value calculated using Eq. (14). The standard deviation of the simulated overall strength is also less than the analytical estimation calculated using Eq. (15), except when the spatial correlation length is very small and the mesh is coarse. This observation suggests that the local averaging method is conservative in terms of variance reduction.

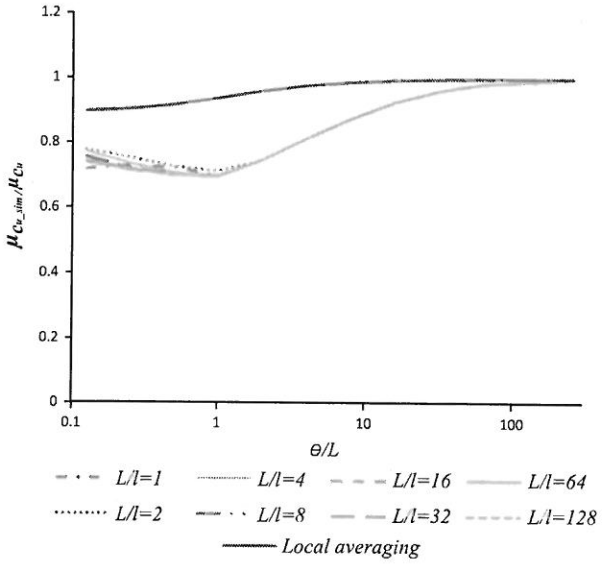

Fig. 10. The mean overall undrained shear strength after the Monte Carlo simulations.

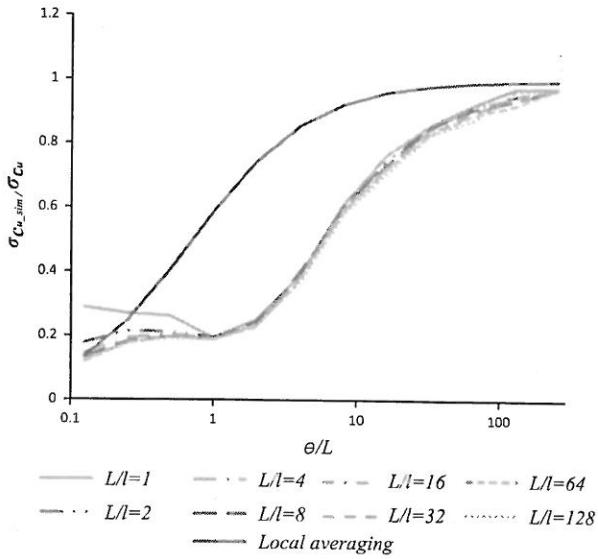

Fig. 11. The standard deviation of the overall undrained shear strength.

4. Concluding remarks

The correct handling of uncertainties in the mechanical properties of engineering materials, particularly geomaterials, is of crucial importance in engineering design. The mechanical properties of soils and rocks may vary spatially, and random field theory is increasingly used by investigators to capture this effect. When using finite element modelling, the question of how small the finite elements need to be to properly characterize the spatial variability arises. Using a statistical approach, this study shows that, due to the "seeking out" effect, the simulated overall mean strength in a biaxial compression test is always less than the locally averaged mean strength. The standard deviation of the simulated overall strength is also less than the standard deviation of the locally averaged strength in most cases.

This study recommends that the element size used in a random finite element analysis be less than half of the spatial correlation length. It is recognized that only the undrained shear strength, 2D random fields and a biaxial compression test have been considered in this study. The recommended element size may be different in more general cases (e.g., frictional materials, 3D models, and softening/hardening materials).

Acknowledgements

The authors wish to acknowledge the support of the Australian Research Council's Centre of Excellence for Geotechnical Science and Engineering.

References

[1] Ahmed A, Soubra AH. Probabilistic analysis at the serviceability limit state of two neighboring strip footings resting on a spatially random soil. Struct Saf 2014;49:2–9.

[2] Ching J, Phoon KK. Mobilized shear strength of spatially variable soils under simple stress states. Struct Saf 2013;41:20–8.
[3] Ching JY, Phoon KK. Effect of element sizes in random field finite element simulations of soil shear strength. Comput Struct 2013;126:120–34.
[4] Ching JY, Phoon KK, Kao PH. Mean and variance of mobilized shear strength for spatially variable soils under uniform stress states. J Eng Mech 2014;140(3):487–501.
[5] Fenton GA, Griffiths DV. Statistics of block conductivity through a simple bounded stochastic medium. Water Resour Res 1993;29(6):1825–30.
[6] Fenton GA, Griffiths DV. Three-dimensional probabilistic foundation settlement. J Geotechn Geoenviron Eng 2005;131(2):232–9.
[7] Fenton GA, Griffiths DV. Risk assessment in geotechnical engineering. Wiley; 2008.
[8] Fenton GA, Vanmarcke EH. Simulation of random-fields via local average subdivision. J Eng Mech – ASCE 1990;116(8):1733–49.
[9] Griffiths DV, Fenton GA. Probabilistic slope stability analysis by finite elements. J Geotechn Geoenviron Eng 2004;130(5):507–18.
[10] Griffiths DV, Fenton GA, Manoharan N. Bearing capacity of rough rigid strip footing on cohesive soil: probabilistic study. J Geotechn Geoenviron Eng 2002;128(9):743–55.
[11] Griffiths DV, Huang JS, Fenton GA. Influence of spatial variability on slope reliability using 2-D random fields. J Geotechn Geoenviron Eng 2009;135(10):1367–78.
[12] Huang J, Griffiths DV. Return mapping algorithms and stress predictors for failure analysis in geomechanics. J Eng Mech 2009;135(4):276–84.
[13] Huang J, Griffiths DV, Fenton GA. Probabilistic analysis of coupled soil consolidation. J Geotechn Geoenviron Eng 2010;136(3):417–30.
[14] Huang J, Griffiths DV, Fenton GA. System reliability of slopes by RFEM. Soils Found 2010;50(3):343–53.
[15] Huang J, Griffiths DV, Lyamin AV, Krabbenhoft K, Sloan SW. Discretization errors of random fields in finite element analysis. Appl Mech Mater 2014;553:405–9.
[16] Huang J, Lyamin AV, Griffiths DV, Krabbenhoft K, Sloan SW. Quantitative risk assessment of landslide by limit analysis and random fields. Comput Geotech 2013;53:60–7.
[17] Jiang SH, Li DQ, Cao ZJ, Zhou CB, Phoon KK. Efficient system reliability analysis of slope stability in spatially variable soils using Monte Carlo simulation. J Geotechn Geoenviron Eng 2015;141(2).
[18] Jiang SH, Li DQ, Zhang LM, Zhou CB. Slope reliability analysis considering spatially variable shear strength parameters using a non-intrusive stochastic finite element method. Eng Geol 2014;168:120–8.
[19] Kim HK, Santamarina JC. Spatial variability: drained and undrained deviatoric load response. Geotechnique 2008;58(10):805–14.
[20] Li D-Q, Jiang S-H, Cao Z-J, Zhou W, Zhou C-B, Zhang L-M. A multiple response-surface method for slope reliability analysis considering spatial variability of soil properties. Eng Geol 2015;187:60–72.
[21] Lloret-Cabot M, Fenton GA, Hicks MA. On the estimation of scale of fluctuation in geostatistics. Georisk: Assess Manage Risk Eng Syst Geohazards 2014;8(2):129–40.
[22] Lyamin AV, Sloan SW, Krabbenhoft K, Hjiaj M. Lower bound limit analysis with adaptive remeshing. Int J Numer Meth Eng 2005;63(14):1961–74.
[23] Ma X, Zabaras N. A stabilized stochastic finite element second-order projection method for modeling natural convection in random porous media. J Comput Phys 2008;227(18):8448–71.
[24] Mollon G, Phoon KK, Dias D, Soubra AH. Validation of a new 2D failure mechanism for the stability analysis of a pressurized tunnel face in a spatially varying sand. J Eng Mech – ASCE 2011;137(1):8–21.
[25] Vanmarcke E. Random fields: analysis and synthesis. World Scientific; 1984.
[26] Zhang DX, Lu ZM. An efficient, high-order perturbation approach for flow in random porous media via Karhunen–Loeve and polynomial expansions. J Comput Phys 2004;194(2):773–94.